



Queensland University of Technology
Brisbane Australia

This is the author's version of a work that was submitted/accepted for publication in the following source:

Frost, Ray L., Xi, Yunfei, Palmer, Sara J., Tan, Keqin, & Millar, Graeme J. (2012) Vibrational spectroscopy of synthetic archerite (K,NH₄)H₂PO₄ : and in comparison with the natural cave mineral. *Journal of Molecular Structure*, 1011, pp. 128-133.

This file was downloaded from: <http://eprints.qut.edu.au/48766/>

© Copyright 2012 Elsevier

This is the author's version of a work that was accepted for publication in <Journal of Molecular Structure>. Changes resulting from the publishing process, such as peer review, editing, corrections, structural formatting, and other quality control mechanisms may not be reflected in this document. Changes may have been made to this work since it was submitted for publication. A definitive version was subsequently published in *Journal of Molecular Structure*, [VOL 1011, (2012)] DOI: 10.1016/j.molstruc.2011.12.013

Notice: *Changes introduced as a result of publishing processes such as copy-editing and formatting may not be reflected in this document. For a definitive version of this work, please refer to the published source:*

<http://dx.doi.org/10.1016/j.molstruc.2011.12.013>

19 INTRODUCTION

20 The minerals archerite originated from the Murra-el-elevyn Cave, Eucla, Western Australia.
21 Archerite $(K,NH_4)(H_2PO_4)$ [1] is commonly found in these cave systems. Another mineral
22 commonly found in these caves is mundrabbillaite $(NH_4)_2Ca(HPO_4)_2 \cdot H_2O$ [2]. Other minerals
23 found in the Murra-el-elevyn Cave and the Petrogale cave include apthitalite
24 $((K,Na)_3Na(SO_4)_2)$, halite (NaCl), syngenite $((K,Na)_3Na(SO_4)_2)$, stercorite
25 $(H(NH_4)Na(PO_4) \cdot 4H_2O)$, oxammite $((NH_4)_2(C_2O_4) \cdot H_2O)$, weddellite $(Ca(C_2O_4) \cdot 2H_2O)$,
26 whitlockite $(Ca_9Mg(PO_4)_6(HPO_4))$, guanine $(C_5H_5N_5O)$, newberyite $(Mg(HPO_4) \cdot 3H_2O)$ and
27 calcite $(CaCO_3)$. These minerals occur as stalactites and form on wall and floor crusts. These
28 minerals are formed through the chemical reactions of calcite with bat guano, or with
29 chemicals from bat guano that are water soluble and crystallise out on the calcite surfaces.
30 The mineral archerite is soluble in cold water and may translocate through the Murra-el-
31 elevyn cave network [3].

32 Some studies on the growth kinetics of archerite have been undertaken [4]; however, these
33 authors state that they are using potassium hydrogen phosphate, but this is not the formula of
34 the mineral archerite. Archerite has the ammonium cation in the structure. An alternative
35 name for the mineral may be biphosphammite [5], a name which is derived from the
36 combination of phosphate and ammonium. Whether archerite and biphosphammite is the
37 same mineral or not is open to question [6]. The crystal structure is close to that of synthetic
38 potassium dihydrogen phosphate [7]. This is not surprising since the size of the potassium
39 and ammonium cations are very close. Some studies of the ferroelectric properties of
40 KH_2PO_4 have been undertaken, which involved structural studies of KH_2PO_4 [8, 9]. Because
41 of the ferroelectric properties of this chemical, there have been some detailed Raman
42 spectroscopic studies of KH_2PO_4 [10-16]. Kim and Choi [12] found broad bands for KH_2PO_4
43 at 1800, 2400 and around 2700 cm^{-1} . These bands were attributed to O...H stretching and
44 bending bands [12]. A detailed study of calcium phosphates including calcium dihydrogen
45 phosphate has been reported [17].

46 The amount of published data on the vibrational spectroscopy of 'cave' minerals including
47 phosphates is quite limited. Further, there is almost no data on the Raman spectroscopy of
48 the phosphate 'cave' minerals. Some studies of phosphate minerals in caves have been
49 undertaken by the authors [6, 18-20]. Raman spectroscopy has proven most useful for the
50 study of mineral structures [21-27]. The objective of this research is to report the Raman and

51 infrared spectra of the synthetic archerite analogue, to compare the spectra of the synthesised
52 archerite and the natural cave mineral and to relate the spectra to the molecular structure of
53 the mineral archerite.

54 **EXPERIMENTAL**

55 **Synthesis of archerite**

56 All starting chemicals: mono-potassium phosphate (KH_2PO_4), mono-ammonium phosphate
57 ($\text{NH}_4\text{H}_2\text{PO}_4$) and phosphoric acid (H_3PO_4 , 85%wt) were from Sigma-Aldrich. A solution of
58 KH_2PO_4 was prepared by adding 27.0967g of KH_2PO_4 to 150ml of water, along with
59 22.9033g of $\text{NH}_4\text{H}_2\text{PO}_4$. This was followed by the addition of 10ml of H_3PO_4 to decrease the
60 pH to about 7. The mixture was stirred continuously for 10 days under ambient conditions
61 until most of the gel like material was crystallised. The whole mixture was transferred to an
62 oven to dry at 105°C overnight.

63 **Mineral**

64 The mineral archerite was supplied by the Australian Museum and originated from Murra-el-
65 elevyn Cave, about 200 km east of Balladonia, Western Australia and also from the Petrogale
66 Cave, Madura, Western Australia. Details of the mineral have been published (page 21) [28].

67 **Raman spectroscopy**

68 Crystals of the archerite analogue were placed on a polished metal surface on the stage of an
69 Olympus BHSM microscope, which is equipped with 10x, 20x, and 50x objectives. The
70 microscope is part of a Renishaw 1000 Raman microscope system, which also includes a
71 monochromator, a filter system and a CCD detector (1024 pixels). The Raman spectra were
72 excited by a Spectra-Physics model 127 He-Ne laser producing highly polarised light at 633
73 nm and collected at a nominal resolution of 2 cm^{-1} and a precision of $\pm 1\text{ cm}^{-1}$ in the range
74 between 100 and 4000 cm^{-1} . Repeated acquisition on the crystals using the highest
75 magnification (50x) was accumulated to improve the signal to noise ratio in the spectra.
76 Spectra were calibrated using the 520.5 cm^{-1} line of a silicon wafer.

77 **Infrared spectroscopy**

78 Infrared spectra were obtained using a Nicolet Nexus 870 FTIR spectrometer with a smart
79 endurance single bounce diamond ATR cell. Spectra over the $4000\text{--}525\text{ cm}^{-1}$ range were

80 obtained by the co-addition of 128 scans with a resolution of 4 cm^{-1} and a mirror velocity of
81 0.6329 cm/s . Spectra were co-added to improve the signal to noise ratio.

82

83 Band component analysis was undertaken using the Jandel 'Peakfit' (Erkrath,
84 Germany) software package which enabled the type of fitting function to be selected and
85 allowed specific parameters to be fixed or varied accordingly. Band fitting was done using a
86 Lorentz-Gauss cross-product function with the minimum number of component bands used
87 for the fitting process. The Lorentz-Gauss ratio was maintained at values greater than 0.7 and
88 fitting was undertaken until reproducible results were obtained with squared correlations (r^2)
89 greater than 0.995. Band fitting of the spectra is quite reliable providing there is some band
90 separation or changes in the spectral profile.

91 **RESULTS AND DISCUSSION**

92 *Background*

93 In aqueous systems, the Raman spectra of phosphate oxyanions show a symmetric stretching
94 mode (ν_1) at 938 cm^{-1} , an antisymmetric stretching mode (ν_3) at 1017 cm^{-1} , a symmetric
95 bending mode (ν_2) at 420 cm^{-1} and a ν_4 bending mode at 567 cm^{-1} [29-31]. S.D. Ross in
96 Farmer (page 404) listed some well-known minerals containing phosphate, which were either
97 hydrated or hydroxylated or both [32]. The vibrational spectrum of the dihydrogen phosphate
98 anion has been reported in Farmer. The PO_2 symmetric stretching mode occurs at 1072 cm^{-1}
99 and the POH symmetric stretching mode at $\sim 878\text{ cm}^{-1}$. The position of the PO stretching
100 vibration for calcium dihydrogen phosphate is found at 915 cm^{-1} . The POH antisymmetric
101 stretching mode is at 947 cm^{-1} and the $\text{P}(\text{OH})_2$ bending mode at 380 cm^{-1} . The band at 1150
102 cm^{-1} is assigned to the PO_2 antisymmetric stretching mode. The position of these bands will
103 shift according to the crystal structure of archerite.

104

105 *X-ray diffraction*

106 The X-ray diffraction patterns of the synthesised archerite analogue and the standard
107 reference pattern are provided in **Figure 1**. Obviously the two patterns are identical, thus
108 proving purer archerite was synthesised. Further the synthesised archerite analogue does not
109 contain any impurity.

110 *Vibrational Spectroscopy*

111 The Raman spectrum of synthetic archerite is displayed in **Figure 2**. The position of this band
112 is in harmony with that reported by Ross in Farmer [32] (Table 17.IX page 396). In aqueous
113 systems, the band is found at 878 cm^{-1} . The infrared spectrum of the archerite analogue is
114 given in **Figure 3**, with infrared bands observed at around 890 and 1080 cm^{-1} . The infrared
115 bands at 1080 and 1115 cm^{-1} are attributed to the ν_3 symmetric PO_2 vibrations, while bands at
116 837 , 894 and 930 cm^{-1} are assigned to the ν_4 $\text{P}(\text{OH})_2$ symmetric stretching vibrations. The
117 spectra of the archerite analogue may be compared with that of the natural mineral. Raman
118 bands of the cave mineral archerite are observed at 981 , 1005 , 1139 and 1165 cm^{-1} . The
119 Raman band at 981 cm^{-1} is assigned to the ν_1 symmetric stretching mode of the POH units,
120 whereas the Raman band at 1005 cm^{-1} is assigned to the ν_1 symmetric stretching mode of the
121 PO_4^{3-} units. Galy [33] first studied the polarized Raman spectra of the H_2PO_4^- anion, while
122 Choi *et al.* reported the polarization spectra of NaH_2PO_4 crystals. Casciani and Condrate
123 [17] published spectra on brushite and monetite together with synthetic anhydrous
124 monocalcium phosphate ($\text{Ca}(\text{H}_2\text{PO}_4)_2$), monocalcium dihydrogen phosphate hydrate
125 ($\text{Ca}(\text{H}_2\text{PO}_4)_2 \cdot \text{H}_2\text{O}$) and octacalcium phosphate ($\text{Ca}_8\text{H}_2(\text{PO}_4)_6 \cdot 5\text{H}_2\text{O}$). These authors
126 determined band assignments for $\text{Ca}(\text{H}_2\text{PO}_4)_2$ and reported bands at 1002 and 1011 cm^{-1} as
127 POH and PO stretching vibrations, respectively. The two Raman bands at 1139 and 1165 cm^{-1}
128 are attributed to both the HOP and PO antisymmetric stretching vibrations. Casciani and
129 Condrate [17] tabulated Raman bands at 1132 and 1155 cm^{-1} and assigned these bands to P-
130 O symmetric and the P-O antisymmetric stretching vibrations. The first assignment, however,
131 differs from what is stated in this work.

132

133 Infrared bands for the cave mineral archerite are found at 980 and 1000 cm^{-1} and at 983 and
134 1002 cm^{-1} for biphosphammite. These bands are attributed to the HOP and PO symmetric
135 stretching vibrations and are the equivalent of the Raman bands at ~ 981 and 1005 cm^{-1}
136 (Casciani and Condrate [17]). Infrared bands are observed at 1021 , 1060 , 1094 , 1139 and
137 1192 cm^{-1} for archerite and at 1025 , 1063 , 1100 , 1140 and 1192 cm^{-1} for biphosphammite.
138 These bands may be attributed to the HOP and PO antisymmetric stretching vibrations.
139 Infrared bands for the mineral dittmarite $(\text{NH}_4)\text{MgPO}_4 \cdot \text{H}_2\text{O}$ are found at 978 , 1063 and 1105
140 cm^{-1} (this work). The infrared bands at 830 and 982 cm^{-1} for archerite and at 843 , 883 and
141 909 cm^{-1} are thought to be associated with the POH deformation modes. Choi *et al.* [34]

142 published spectra of NaH_2PO_4 ; however these authors did not tabulate or mark the position of
143 the peaks. Therefore, it is very difficult to make any comparison of the peak positions of
144 archerite and that of published data by Choi *et al.* Casciani and Condrate [17] reported bands
145 assigned to these vibrational modes for $\text{Ca}(\text{H}_2\text{PO}_4)_2$ at 876 and 901 cm^{-1} .

146

147 The Raman spectrum of archerite analogue in the 100 to 700 cm^{-1} region is displayed in
148 **Figure 4**. Raman bands are observed at 533 and 562 cm^{-1} . These bands are attributed to the
149 ν_4 out of plane bending modes of the H_2PO_4 units. The Raman spectrum of NaH_2PO_4 shows
150 Raman bands at 526, 546 and 618 cm^{-1} . Raman bands are found at 620, 637, 643 and 660
151 cm^{-1} for the cave mineral archerite. Raman bands are determined at 461 and 477 cm^{-1} .
152 These bands are attributed to the ν_2 H_2PO_4 bending modes. Raman bands are observed at
153 429, 441 and 492 cm^{-1} for the cave mineral archerite. The Raman spectrum of NaH_2PO_4
154 shows Raman bands at 460 and 482 cm^{-1} . Intense Raman bands are observed at 347 and 593
155 cm^{-1} assigned to metal-oxygen vibrations. Other Raman bands are observed at 144, 180 and
156 270 cm^{-1} , and are simply described as external vibrations or lattice modes.

157

158 The Raman spectrum of the archerite analogue in the 2800 to 3600 cm^{-1} region is shown in
159 **Figure 5**. A broad spectral envelope is observed, which may be resolved into component
160 bands at 3018, 3089, 3151, 3191, 3235 cm^{-1} . These bands are attributed to water stretching
161 vibrations. These band assignments are supported by the 1660 cm^{-1} band in the water
162 bending region (**Figure 6**). Additional bands at 1421 and 1704 cm^{-1} are attributed to the
163 NH_4^+ bending modes. The Raman bands at 1283, 1409, 1443 and 1546 cm^{-1} for the natural
164 cave mineral archerite are assigned to these bending modes. The bands at around 1406 and
165 1444 cm^{-1} are assigned to the doubly degenerate ν_2 modes, whereas the band at around 1283
166 cm^{-1} is assigned to the ν_4 modes. The observation of so many bands in the ammonium ion
167 bending region indicates that the ammonium ion is strongly distorted in the archerite structure
168 and probably has C_s symmetry.

169

170 The infrared spectrum of the archerite synthetic analogue is shown in **Figure 7**. A broad
171 infrared band centred upon 1620 cm^{-1} may be deconvoluted into component bands at 1545,
172 1606 and 1712 cm^{-1} . These bands are assigned to the deformation modes of the ammonium

173 ion and a water bending vibration. Infrared bands are observed in two sets: the first set is
174 comprised of bands at 1388, 1407, 1426 and 1445 cm^{-1} , and a second set at 1240, 1278 and
175 1303 cm^{-1} . The first set is assigned to NH_4^+ ν_2 bending modes and the second set to NH_4^+ ν_4
176 bending modes. In the infrared spectrum of protiated dittmarite $((\text{NH}_4)\text{MgPO}_4 \cdot \text{H}_2\text{O})$ bands
177 are observed at 1663, 1536, 1482 and 1432 cm^{-1} with a shoulder at 1472 cm^{-1} . Infrared bands
178 are observed at 2099, 2272 and 2387 cm^{-1} for the cave mineral archerite. These bands are
179 attributed to the symmetric stretching vibrations of the hydroxyl units of H_2PO_4^- ions. The
180 observation of multiple bands supports the concept of the non-equivalence of dihydrogen
181 units in the archerite structure. In the infrared spectrum of NaH_2PO_4 , bands are found at
182 2290, 2379, 2682 and 2777 cm^{-1} . Casciani and Condrate [17] reported the infrared bands of
183 $\text{Ca}(\text{H}_2\text{PO}_4) \cdot \text{H}_2\text{O}$ at 2310, 2400 and 2900 cm^{-1} and assigned these bands to the hydroxyl
184 stretching vibrations of the hydroxyls of the H_2PO_4^- units. Infrared bands are observed at
185 2674, 2852, 2921, 3070, 3153, 3252, 3308 and 3374 cm^{-1} for the cave mineral archerite. The
186 latter three bands are attributed to the OH stretching vibrations of water. The first two bands
187 are associated with the stretching vibrations of POH units of the dihydrogen phosphate anion,
188 while the infrared bands at 3070 and 3153 cm^{-1} are attributed to NH stretching vibrations.

189 **CONCLUSIONS**

190 The mineral archerite is an ammoniated hydrogen potassium phosphate commonly found in
191 caves in Western Australia, such as the Petrogale Cave and in the Murra-el-elevyn Cave.
192 However, archerite has been found in many caves worldwide. The synthetic analogue of
193 archerite has been synthesised and the spectra of the natural cave mineral has been compared
194 with the synthetic analogue. X-ray diffraction patterns prove the synthesised compound was
195 indeed archerite. The minerals are formed by the reaction of chemicals from bat (or bird)
196 guano on calcite surfaces. The mineral is associated with other phosphate minerals including
197 struvite, stercorite and brushite. According to Platford [3], the mineral is formed from
198 solution. Hence, the basic components of the mineral can be translocated through a cave
199 system.

200 The individual vibrating units of these minerals lends itself to vibrational spectroscopy. A
201 combination of Raman and infrared spectroscopy has been used to identify vibrational modes
202 associated with the mineral archerite. Raman spectroscopy proves the anion in the synthetic
203 archerite analogue is the dihydrogen phosphate anion. No observation of phosphate or
204 hydrogen phosphate units was found in the archerite analogue. The Raman spectra of the

205 natural cave mineral archerite shows the presence of both the dihydrogen and mono hydrogen
206 phosphate units.

207

208 **Acknowledgments**

209 The financial and infra-structure support of the Queensland University of Technology,
210 Chemistry discipline is gratefully acknowledged. The Australian Research Council (ARC) is
211 thanked for funding the instrumentation.

212

213

214 **References**

- 215 [1] P.J. Bridge, *Mineralogical Magazine* 41 (1977) 33.
 216 [2] P.J. Bridge, R.M. Clark, *Mineralogical Magazine* 47 (1983) 80.
 217 [3] R.F. Platford, *Journal of Chemical and Engineering Data* 19 (1974) 166.
 218 [4] T.N. Thomas, T.A. Land, M. Johnson, W.H. Casey, *Journal of Colloid and Interface*
 219 *Science* 280 (2004) 18.
 220 [5] M.W. Pryce, *Mineralogical Magazine* 38 (1972) 965.
 221 [6] R.L. Frost, Y. Xi, S.J. Palmer, *J. Mol. Struct.* 1001 (2011) 49.
 222 [7] J. West, *Zeitschrift fuer Kristallographie, Kristallgeometrie, Kristallphysik,*
 223 *Kristallchemie* 74 (1930) 306.
 224 [8] B.C. Frazer, R. Pepinsky, *Physical Review* 85 (1952) 479.
 225 [9] B.C. Frazer, R. Pepinsky, *Acta Crystallographica* 6 (1953) 273.
 226 [10] J.P. Coignac, H. Poulet, *Journal de Physique (Paris)* 32 (1971) 679.
 227 [11] E. Courtens, *Solid State Communications* 45 (1983) 479.
 228 [12] J.J. Kim, B.K. Choi, *Raman Spectrosc., Proc. Int. Conf., 8th* (1982) 465.
 229 [13] T. Shigenari, Y. Takagi, *Journal of the Physical Society of Japan* 31 (1971) 312.
 230 [14] I. Takenaka, Y. Tominaga, S. Endo, M. Kobayashi, *Solid State Communications* 84
 231 (1992) 931.
 232 [15] Y. Tominaga, H. Urabe, *Ferroelectrics* 39 (1981) 1021.
 233 [16] T. Yagi, *Nippon Butsuri Gakkaishi* 46 (1991) 591.
 234 [17] F.S. Casciani, R.A. Condrate, Sr., *Proceedings - International Congress on*
 235 *Phosphorus Compounds 2nd* (1980) 175.
 236 [18] R.L. Frost, S.J. Palmer, *Spectrochim. Acta, Part A* 79 (2011) 1215.
 237 [19] R.L. Frost, S.J. Palmer, R.E. Pogson, *Spectrochim. Acta, Part A* 79 (2011) 1149.
 238 [20] R.L. Frost, S.J. Palmer, Y. Xi, *Spectrochim. Acta, Part A* 82 (2011) 132.
 239 [21] R.L. Frost, *J. Raman Spectrosc.* 42 (2011) 540.
 240 [22] R.L. Frost, S.J. Palmer, *J. Mol. Struct.* 988 (2011) 47.
 241 [23] R.L. Frost, S.J. Palmer, H.J. Spratt, W.N. Martens, *J. Mol. Struct.* 988 (2011) 52.
 242 [24] R.L. Frost, S.J. Palmer, Y. Xi, *J. Mol. Struct.* 1001 (2011) 43.
 243 [25] R.L. Frost, S.J. Palmer, Y. Xi, *J. Mol. Struct.* 1004 (2011) 88.
 244 [26] R.L. Frost, Y. Xi, S.J. Palmer, *J. Mol. Struct.* 1001 (2011) 56.
 245 [27] S.J. Palmer, R.L. Frost, *J. Mol. Struct.* 994 (2011) 283.
 246 [28] J.W. Anthony, R.A. Bideaux, K.W. Bladh, M.C. Nichols, *Handbook of Mineralogy*
 247 *Vol.IV. Arsenates, phosphates, vanadates - Mineral Data Publishing, Tucson, Arizona.*
 248 *Mineral data Publishing, Tucson, Arizona, 2000.*
 249 [29] R.L. Frost, W. Martens, P.A. Williams, J.T. Kloprogge, *Mineralogical Magazine* 66
 250 (2002) 1063.
 251 [30] R.L. Frost, W.N. Martens, T. Kloprogge, P.A. Williams, *Neues Jahrbuch fuer*
 252 *Mineralogie, Monatshefte* (2002) 481.
 253 [31] R.L. Frost, P.A. Williams, W. Martens, J.T. Kloprogge, P. Leverett, *Journal of Raman*
 254 *Spectroscopy* 33 (2002) 260.
 255 [32] V.C. Farmer, *Mineralogical Society Monograph 4: The Infrared Spectra of Minerals.*
 256 1974.
 257 [33] A. Galy, *Journal de Physique et le Radium* 12 (1951) 827.
 258 [34] B.K. Choi, M.N. Lee, J.J. Kim, *Journal of Raman Spectroscopy* 20 (1989) 11.

259
260

261

262 **List of Figures**

263 Figure 1 X-ray diffraction patterns of the synthesised archerite analogue and the standard
264 reference pattern

265 Figure 2 Raman spectrum of the synthesised archerite analogue in the 650 to 1250 cm^{-1}
266 region.

267 Figure 3 Infrared spectrum of the synthesised archerite analogue in the 500 to 1200 cm^{-1}
268 region.

269 Figure 4 Raman spectrum of the synthesised archerite analogue in the 100 to 700 cm^{-1} region.

270 Figure 5 Raman spectrum of the synthesised archerite analogue in the 2800 to 3500 cm^{-1}
271 region.

272 Figure 6 Raman spectrum of the synthesised archerite analogue in the 1300 to 1900 cm^{-1}
273 region.

274 Figure 7 Infrared spectrum of the synthesised archerite analogue in the 1200 to 1900 cm^{-1}
275 region.

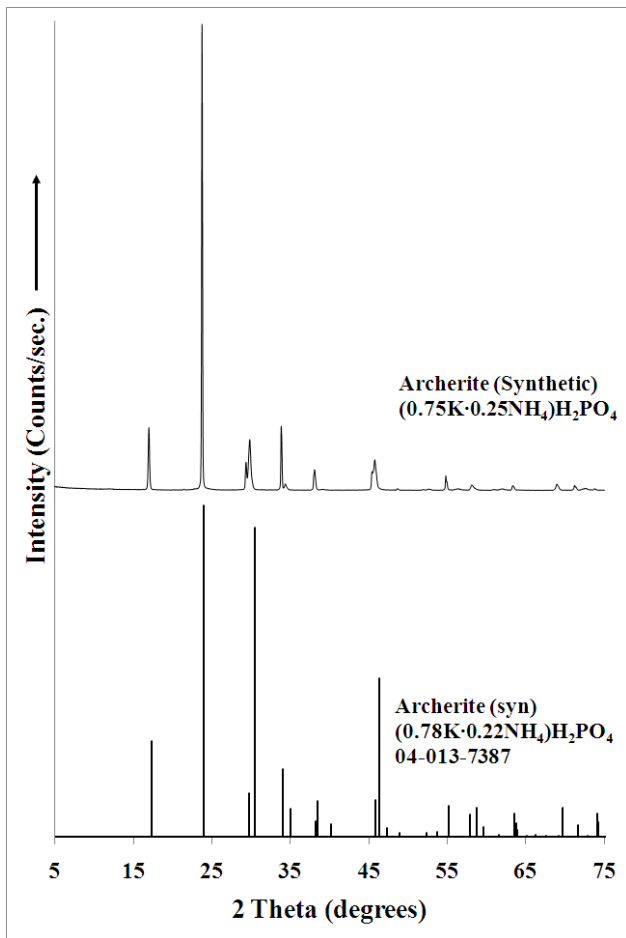
276

277

278

279

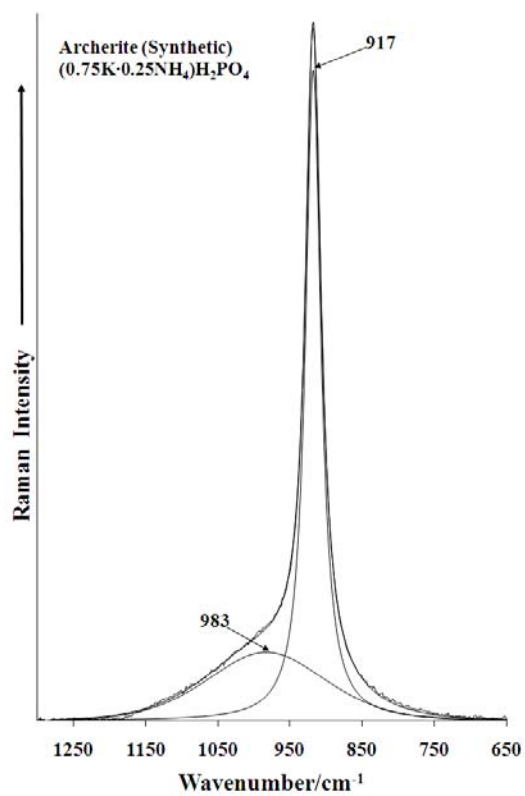
280



281

282 **Figure 1**

283



284

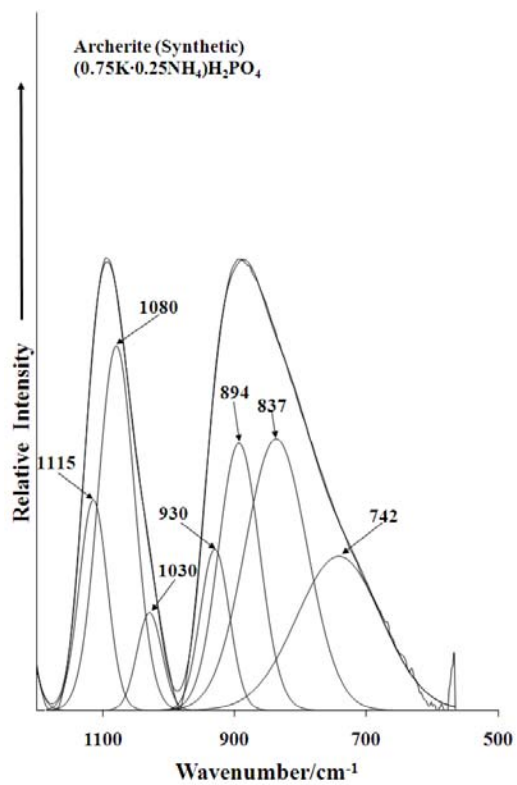
285

286 **Figure 2**

287

288

289



290

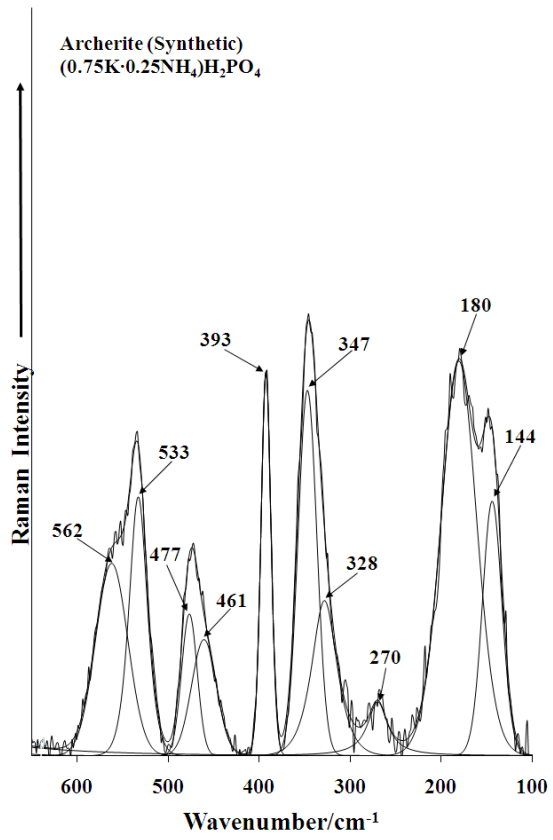
291

292 **Figure 3**

293

294

295



296

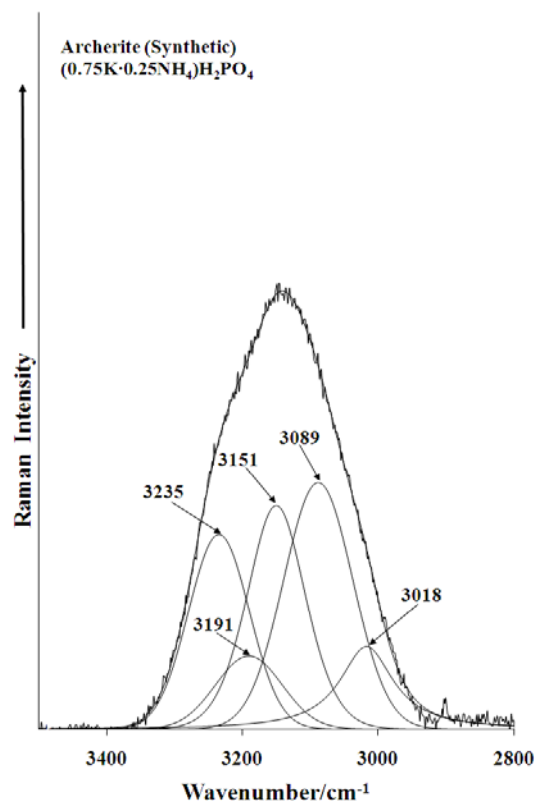
297 **Figure 4**

298

299

300

301



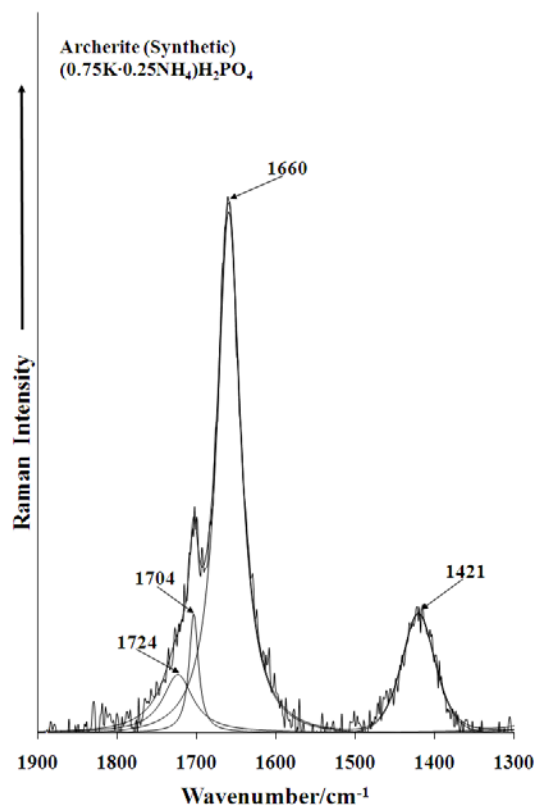
302

303

304 **Figure 5**

305

306

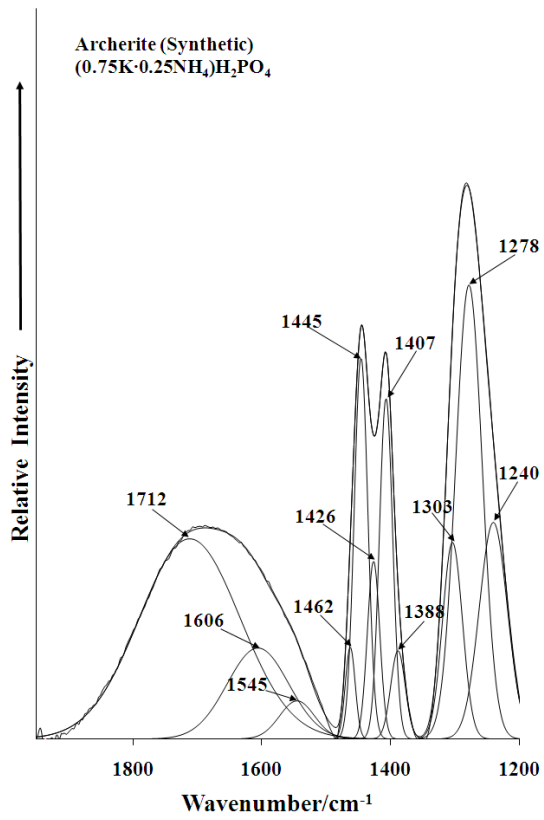


307

308

309 **Figure 6**

310



311

312

313 **Figure 7**

314